

UKAEA-CCFE-PR(20)76

E. Lazzaro, L. Bonalumi, S. Nowak, D. Brunetti

# **On monitoring tearing modes stability in toroidally rotating tokamak equilibria**

Enquiries about copyright and reproduction should in the first instance be addressed to the UKAEA Publications Officer, Culham Science Centre, Building K1/O/83 Abingdon, Oxfordshire, OX14 3DB, UK. The United Kingdom Atomic Energy Authority is the copyright holder.

The contents of this document and all other UKAEA Preprints, Reports and Conference Papers are available to view online free at [scientific-publications.ukaea.uk/](https://scientific-publications.ukaea.uk/)

# **On monitoring tearing modes stability in toroidally rotating tokamak equilibria**

E. Lazzaro, L. Bonalumi, S. Nowak, D. Brunetti



12345

# On monitoring tearing modes stability in toroidally rotating tokamak equilibria

E. Lazzaro, L. Bonalumi, S. Nowak, Brunetti

**Abstract**—In tokamak operation the control of dangerous MHD instabilities, possibly in r-t scenarios, must rely on prompt robust diagnostics of the state and stability of the system. The set of magnetic signals measured on the outside of the plasma boundary, based on the Zakharov-Shafranov, Shkarowsky, Wootton (ZSSW) [5] current moments has been always used for reliable monitoring of key characteristics of the instantaneous equilibrium condition, such as the quantities  $\Delta_h$ , the Shafranov centroid shift,  $\beta_p$  related to the thermal energy content, and  $l_i$  related to the current profile peakedness. In addition the fast pick up coils monitor the external magnetic field fluctuations due to internal MHD activity, however without possibility of radial localization of the source. Here we explore the potential usefulness of a more complete use of ZSSW moments in association with the information from fast B perturbation signals to detect tearing stability conditions. For clarity we set up an analysis of the measurable response to tearing perturbations based on an exact equilibrium model, which is an extension of the Solov'ev case with the addition of an equilibrium, non uniform plasma rotation  $\Omega(\psi)$ . The relation of selected (externally measurable) ZSSW moments to the calculated stability index, is mapped for different rotation values. The footprint of the stability condition  $\Delta' < 0$  on some current moments on the outer surface [5], [14] can then identify stability boundaries, for different rotation conditions. This first discussion on an idealized exact model is proposed for testing the concept for application to realistic equilibria, since it relies on few, externally monitorable quantities and very basic assumptions on the tearing modes physics.

**Index Terms**—tokamak, current moments, tearing modes, Bayes observer

## I. INTRODUCTION

**T**HIS work offers a contribution to the question of robust identification of some tokamak magnetic instabilities, which is crucial for the successful operation of the fusion oriented devices. Although the argument is based on well known and well developed physics, it is helpful for the reader to start with a, non pedantic, concise summary of the relevant equilibrium conditions, and basic description of the tearing instability considered. Therefore in the second Section the notation is established, and a general tokamak equilibrium equation is derived a-new including a steady rotation; the third Section contains the explicit solution of a Solov'ev type and its transformation to a parametric representation that allows easy construction of the metrics and identification of physical and geometric properties. In the next Section, the

specific reconnection process at rational surfaces is succinctly described, focussing on the specific toroidal metrics effects on the current perturbation giving rise to the instability. The crucial argument on the scaling of the source of the instability is introduced and discussed. On this basis in the subsequent Section the concept of external magnetic measurements is revisited and extended; the solution of the homogeneous Grad-Shafranov equation in spherical coordinates is recalled to generate Zakharov-Shafranov, Shkarowsky, Wootton (ZSSW) [5] current moments; the relation of generalized (externally measurable) ZSSW moments to the calculated stability index  $\Delta'$ , is mapped for different rotation values. The footprint of the stability condition  $\Delta' < 0$  on some current moments on the outer surface [5], [14] can then identify stability boundaries, for different rotation conditions. The simplicity of the physical assumptions is believed to constitute a ground model which can be improved but not contradicted by more complete descriptions of the inner profiles. In the last section a Bayesian inference approach is used to test the theoretical detectability of the relevant information amidst the other measurements. In the conclusions, this first example based on an idealized analytical model is proposed for testing the method in view of application to realistic equilibria, since it relies on few, externally monitorable quantities and very basic assumptions on the T.M. physics.

## II. BASIC EQUILIBRIUM FRAMEWORK

The purpose of this work is to explore and eventually propose an extended use of the magnetic measurements taken *outside* the Last Closed Magnetic Surface (LCMS) of a tokamak, to contribute means of continuous monitoring of the stability conditions of the configuration relative, in a first instance, to tearing perturbations. In order to set up the problem as clearly as possible we find convenient to choose as demonstrative playground the geometry of the simplest, albeit not fully realistic, tokamak equilibrium, namely a variant of the Solov'ev type [1], [2]. In particular we first re-derive a solution of the Grad-Shafranov equation, including in the equilibrium a non uniform toroidal rotation, and cast the solution in the inverse coordinate parametric representation which highlights simply the geometric characteristics of the configuration. The first step is to consider the steady state, incompressible single fluid MHD equations

$$\rho(\mathbf{v} \cdot \nabla \mathbf{v}) = \mathbf{J} \times \mathbf{B} - \nabla p \quad (1)$$

$$-\nabla \Phi + \mathbf{v} \times \mathbf{B} = \mathbf{0} \quad (2)$$

$$\nabla \cdot (\rho \mathbf{v}) = 0 \quad (3)$$

E. Lazzaro is Associate at the Institute for Science and Technology of Plasma (ISTP) of the Consiglio Nazionale delle Ricerche, Via Cozzi 53, Milan 20125 Italy, e-mail: (enzo.lazzaro@ist.cnr.it).

L. Bonalumi was with University of Milan-Bicocca.

S. Nowak is First Researcher at ISTP-CNR, Milan.

D. Brunetti is Researcher at CCFE, Culham, UK.

Manuscript received April 19, 2005; revised August 26, 2015.

where the second equation represents Ohm's law, with  $\Phi$  the electrostatic potential. Due to axisymmetry and the incompressibility condition, the  $\mathbf{B}$  field and the mass density flow can be written in the Clebsch notation as:

$$\mathbf{B} = T\nabla\phi + \nabla\phi \times \nabla\psi \quad (4)$$

$$\rho\mathbf{v} = \Theta\nabla\phi + \nabla\phi \times \nabla F \quad (5)$$

Here  $T, F, \Theta, \Phi$  are all functions of the poloidal flux  $\psi(R, Z)$ , therefore are *constant on magnetic surfaces*. Using expressions 5 in equations 1, with straightforward algebra one obtains:

$$\Phi' = \frac{1}{\rho R^2} [TF' - \Theta] \quad (6)$$

The projection of the momentum balance equation 1 along the  $\nabla\phi$  direction, yields another surface quantity, from which a final expression for the flow velocity follows:

$$X(\psi) = T\left(1 - \frac{(F')^2}{\rho}\right) + R^2 F' \Phi' \quad (7)$$

$$\mathbf{v} = \frac{F'}{\rho} \mathbf{B} \nabla\phi - R^2 \Phi' \nabla\phi \quad (8)$$

The projection of the momentum balance equation 1 along  $\mathbf{B}$  vanishes, and equations 6,8 yield the following relations:

$$\mathbf{B} \cdot \left[ \frac{1}{2} (\nabla v^2) + \frac{\Phi'}{\rho} (F'T - \Phi' \rho R^2) + \frac{\nabla p}{\rho} \right] = 0 \quad (9)$$

Finally the last equation 9 can be rewritten, using equation 6, as a generalized Bernoulli equation

$$\mathbf{B} \cdot \nabla \left[ p + \rho \left( \frac{v^2}{2} + \Phi' \frac{\Theta}{\rho} \right) \right] = 0 \quad (10)$$

The quantity  $P_s(\psi) = p + \rho \left( \frac{v^2}{2} + \Phi' \frac{\Theta}{\rho} \right)$  is a surface function ; it is convenient to introduce the *poloidal Mach number*  $M^2 \equiv \frac{v_p^2}{v_A^2} = \frac{(F')^2}{\rho}$  and write the projection of the momentum balance equation in the  $\nabla\psi$  direction, obtaining the Grad-Shafranov equation generalized with the presence of a stationary toroidal plasma velocity  $v_\phi = \Theta/R\rho$ :

$$(1 - M^2) \Delta^* \psi - \frac{(M^2)'}{2} |\nabla\psi|^2 + \frac{1}{2} \left( \frac{X^2}{1 - M^2} \right)' + R^2 \left( P_s - \frac{XF'\Phi'}{1 - M^2} \right)' + \frac{R^4}{2} \left( \frac{\rho(\Phi')^2}{1 - M^2} \right)' = 0 \quad (11)$$

The Beltrami operator is explicitly  $\Delta^* \psi = \frac{\partial^2 \psi}{\partial R^2} - \frac{2}{R} \frac{d\psi}{dR} + \frac{\partial^2 \psi}{\partial Z^2}$ . In absence of equilibrium flow, the Grad-Shafranov equation, and the toroidal current density are:

$$\Delta^* \psi = -\mu_0 R J_\phi \quad J_\phi = R \frac{dp}{d\psi} + \frac{T}{2\pi\mu_0 R} \frac{dT}{d\psi} \quad (12)$$

In the following we shall consider just the subsonic cases  $M^2 \ll 1$  for which the equation 11 remains elliptic. Comparison of eq.11 and eq. 12 in the subsonic range, leads to identify the current density in presence of rotation:

$$J_\phi = -\frac{1}{2\mu_0 R} (X^2)' + R(P_s - XF'\Phi')' + \frac{R^3}{2} (\rho(\Phi')^2)' \quad (13)$$

### A. Paradigmatic Case with Exact Solution

In this section eqs.13 and 11, will be simplified choosing particular profiles. Although they might not picture a realistic situation, they provide a clear insight in the role and effects of the configuration geometry. In the following we shall be concerned with *external* measurements, which are generally considered rather "blind" to the internal features, but we can show that even the coarse description used can provide general conclusions. Noting that  $X \rightarrow T$  and choosing

$$F' = 0 \quad (14)$$

$$T = \text{const} \quad (15)$$

$$\omega(\psi) = \frac{\Theta(\psi)}{\rho R^2} = -\Phi'(\psi) \quad (16)$$

$$p = p_0 \left(1 - \frac{\psi}{\psi_b}\right) \quad (17)$$

$$\rho\omega^2 = \Omega_0 \left(1 - \frac{\psi}{\psi_b}\right) \quad (18)$$

$$\Omega = \mu_0 \Omega_0 / 2\psi_b \quad (19)$$

$$P_0 = \mu_0 p_0 / \psi_b \quad (20)$$

where  $[P_0] = [\mu_0 J l^{-1}]$  and  $[\Omega = \mu_0 \Omega_0 / 2\psi_b] = [\mu_0 l^{-5} q t^{-1} \approx \mu_0 J l^{-3}]$  labels the rotation effect on the current density; the equation 12 becomes:

$$\Delta^* \psi = -R^2 P_0 - R^4 \Omega \quad (21)$$

Following the classical procedure by Solov'ev [1] an exact solution is obtained in the form

$$\psi(R, Z) = c_0 R^2 Z^2 + k(R^2 - R_0^2)^2 + \alpha R^\beta \quad (22)$$

After further de-dimensionalization of eq.21, the coefficients and the final form of the solution are obtained, assigning boundary conditions  $\psi = \psi_b = 4kR_0^2 r_b^2$ , going through the points  $r = r_b$ ,  $Z = Z_s = Z(r_b, \pi/2)$  and vanishing on the magnetic axis. With  $k = \frac{Z_s \sqrt{\mu_0 p_0}}{4R_0 r_b \sqrt{2(Z_s^2 + r_b^2)}}$ ,  $c_0 = \frac{8r_b^2}{Z_s^2} k$  one gets:

$$\psi(R, Z) = c_0 R^2 Z^2 + k(R^2 - R_0^2)^2 + \frac{\Omega}{24} R^6 - \psi_{ax} \quad (23)$$

The last constant makes the flux vanish at the magnetic axis, and is  $\psi_{ax} = \frac{\Omega}{24} R_0^6 - \frac{\Omega^2}{256k} R_0^8$ . The poloidal  $B_\theta$  field in rectified flux coordinates  $(r, \theta, \phi)$  is  $B_\theta(r) = \frac{\psi'(r)}{\sqrt{g}}$  where  $\sqrt{g}$  is the Jacobian of the transformation from the  $(R, \phi, Z)$  coordinates. A simple but crucial observation should be made on the structure of the current density on the r.h.s. of eq.21. It is basically an expression of the fundamental force balance in *toroidal geometry*, and is strictly related to the geometric and global properties of the equilibrium configuration, which are efficiently identified by "moments" measured outside the plasma; toroidicity and shaping help removing certain degeneracies, allowing for instance separation of  $\beta_p$  and  $\ell_i$  [4], [15]. A first conjecture, is that this "irreducible" toroidal effect may carry also other global information, so far disregarded, related to certain stability conditions.

### B. Parametric Representation of Exact Solution and Metric Coefficients

The exact solution 23 can be usefully represented in the general parametric form [3]

$$R(r, \theta) = R_{ax} + (R_1(r) + R_{11}(r, \Omega))\cos\theta + R_2(r)\cos 2\theta - \delta \quad (24)$$

$$Z(r, \theta) = (Z_1(r) + Z_{11}(r, \Omega))\sin\theta \quad (25)$$

Here  $r$  is a flux surface function, and  $\theta$  is a rectified poloidal angle variable. From eqs. 24 and 25 the metric tensor  $g_{ik}$  is easily calculated analytically, to be used in writing the equation for the helical magnetic perturbations, in full toroidal geometry. For simplicity we show in the Appendix the explicit expressions of the coefficients of eqs. 24 and 25, and display the relevant metrics later on when needed. A fair amount of tedious algebra is unavoidable to be able to evaluate consistently some moments of the interior current profile and some contour integrals on the plasma outer boundary, thereby proving our statements, anticipated in the introduction.

### III. EXTERNAL MAGNETIC MEASUREMENTS

The tokamak toroidal current density distribution,  $J_\phi(\mathbf{r})$  is a continuous function of points  $\mathbf{r}$  of coordinates  $(R, Z)$ , compact within the domain (set of points)  $S$  bounded by the Last Closed Magnetic Surface (LCMS). For convenience, in the following we shall use the normalized profile  $\hat{J}_\phi(\mathbf{r}) \simeq J_\phi(\mathbf{r})S_\phi/I$ , where  $I$  is the total current and  $S_\phi$  a toroidal cross section. Consider a complete numerable set  $\mathfrak{R}$  of real valued orthonormal basis functions  $u_n(\mathbf{r})$ ; the normalized function  $\hat{J}_\phi(\mathbf{r})$  could be represented by an expansion in  $u_n(\mathbf{r})$ , in the form of a smooth (integral) superposition of *filaments*:

$$\hat{J}_\phi(\mathbf{r}) = \int d\mathbf{r}' \sum_n C_n u_n(r') \delta(\mathbf{r} - \mathbf{r}') \quad (26)$$

and the reconstruction of the current profile, albeit approximate, in principle could be expected to consist in determining the weighting coefficients  $C_n$  by finding a large enough number  $N$  of external measurements to be matched to  $N$  boundary values of  $u_n(\mathbf{r}_b)$ , obviously under the constraint that  $\sum_n C_n u_n(\mathbf{r}_b) = \mathbf{0}$ , with the integral value constrained by the measured total current  $I$ . However this procedure cannot be *even formally* pursued, outside the general formulation of a suitably regularized inverse MHD equilibrium problem [13]. The use of external magnetic diagnostics has nonetheless proved to be a powerful and robust tool to determine several important characteristics of the tokamak configuration, such as the plasma position and shape, associated to the  $J_\phi$  profile and the boundary conditions. Zakharov and Shafranov [4], [5] first showed that multipole moments of current density are given by closed-contour integrals of external magnetic field and how these moments are related to plasma position and shape. Their analysis limited to the case of symmetry with respect to the midplane and first order in  $\epsilon = r/R$ , was later expanded by other authors [6]–[9], always with the objective of a robust identification of the geometrical characteristics of the plasma meridian cross section. In the

work by [5], [7]–[9], the solution of the homogeneous Grad-Shafranov equation, valid in vacuum is expressed in terms functions of the type  $f^{(m)}(\rho, \mu) = \rho^{m+1}(1 - \mu^2)^{1/2}P_m^1(\mu)$  (where  $\rho^2 = R^2 + Z^2, \mu = \cos\theta$ ), related to associated Legendre polynomials, and it is shown that  $m$ -th moments of the internal current profile  $J_\phi$ , defined in [5], [8], [9], are equal to weighted contour integrals of the peripheral magnetic field tangent and normal components on closed paths, surrounding the plasma:

$$Y_m = \frac{1}{\mu_0 I} \int J_\phi f_m dS_\phi = \frac{1}{\mu_0 I} \oint f_m B_\theta(r_b) dl$$

$$= \frac{1}{\mu_0 I} \int_0^{2\pi} f_m B_\theta(r_b) \sqrt{g_{\theta\theta}(r_b)} d\theta \quad (27)$$

For convenience the set of functions  $f^{(m)}(R, Z)$  is changed into an equivalent set  $f_m(x, Z)$  vanishing on the magnetic axis, and for the sake of argument the integration contour is the plasma boundary, at  $r = r_b$ . In the following the moments 27 of interest shall be those generated by the functions of ref. [9]:

$$f_1 = x(1 + \frac{x}{R_0}) \quad (28)$$

$$f_2 = xZ(1 + \frac{x}{R_0})^2 \quad (29)$$

$$f_3 = x^2(1 + \frac{x}{2R_0})^2 - Z^2(1 + \frac{x}{R_0}) \quad (30)$$

$$f_4 = [2Zx(1 + \frac{x}{2R_0}) - \frac{4}{3}\frac{Z^3}{R_0}](1 + \frac{x}{R_0})^2 \quad (31)$$

$$f_5 = x^3(1 + \frac{x}{2R_0})^3 - 3xZ^2(1 + \frac{x}{2R_0})(1 + \frac{x}{R_0})^2 \quad (32)$$

$$f_6 = [3Zx^2(1 + \frac{x}{2R_0})^2 - Z^3(1 + \frac{6x}{R_0} + \frac{3x^2}{R_0^2})](1 + \frac{x}{R_0})^2 \quad (33)$$

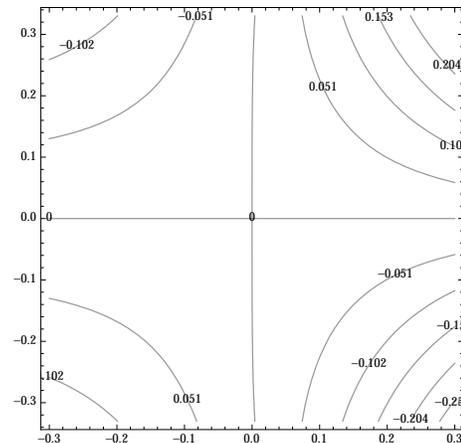


Fig. 1. Contour plot in  $(x, Z)$  plane, of  $f_4$  multipolar function, associated with the elongation  $\kappa$

### IV. LINEAR TEARING MODES PERTURBATIONS

First order helical perturbations of the type  $\tilde{f}(r, \theta, \phi) = \tilde{f}(r)_{m,n} e^{i(m\theta - n\phi)}$  in current density may lead to magnetic instabilities growing around the closed field lines, rational  $q$  surfaces and generating the externally measured, time

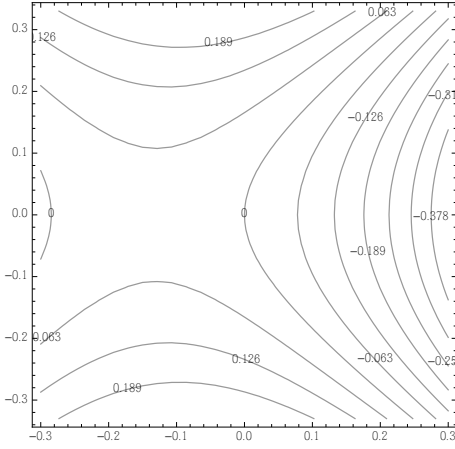


Fig. 2. Contour plot in  $(x,Z)$  plane, of  $f_{\Delta}$  multipolar function

periodic "Mirnov" signals. Eventually the instability transforms nonlinearly in finite size magnetic islands, whose evolution, up to the saturation stage, largely depends on the linear growth rate. The latter is governed by a dispersion relation of the type

$$\Delta' = \Delta'_{layer} \quad (34)$$

where  $\Delta'_{layer}$  depends on the physics of magnetic reconnection within the inner layer around  $r=r(q=m/n)$ , and the "external"  $\Delta' = \frac{d \ln(\tilde{\psi}_{m,n})}{dr} |_{r(q=m/n)}$  results from the solution of the tearing equation. Considering linear perturbations of current and magnetic field

$$\mathbf{J} = \mathbf{J}_0 + \tilde{\mathbf{J}}_1 \quad (35)$$

$$\mathbf{B} = \mathbf{B}_0 + \tilde{\mathbf{B}}_1 \quad (36)$$

The condition of vanishing torque density  $\nabla \times (\mathbf{J} \times \mathbf{B}) = 0$  is expressed in the equation for the first order perturbed helical poloidal flux  $\tilde{\psi}_{m,n}$ , which in curvilinear (toroidal) geometry takes the form:

$$\begin{aligned} & \left\langle \frac{g_{\theta\theta}}{\sqrt{g}} \right\rangle \frac{\partial^2 \tilde{\psi}_{m,n}}{\partial r^2} + \left\langle \frac{g_{\theta\theta}}{\sqrt{g}} \right\rangle' \frac{\partial \tilde{\psi}_{m,n}}{\partial r} \\ & - [m^2 \left\langle \frac{g_{rr}}{\sqrt{g}} \right\rangle + \frac{m}{m-nq} \langle J^* \rangle'] \tilde{\psi}_{m,n} = 0 \end{aligned} \quad (37)$$

In explicit form, in this basic configuration, we have the following dependence on the geometry, pressure and rotation:

$$\left\langle \frac{g_{\theta\theta}}{\sqrt{g}} \right\rangle = \frac{4\sqrt{2}r(c_0 + 8k)}{33R_0\sqrt{c_0k}} + \frac{\Omega R_0 r(c_0 + 8k)}{44\sqrt{2}c_0k^3} \quad (38)$$

$$\left\langle \frac{g_{\theta\theta}}{\sqrt{g}} \right\rangle' / \left\langle \frac{g_{\theta\theta}}{\sqrt{g}} \right\rangle = \frac{1}{r} \quad (39)$$

$$\left\langle \frac{g_{rr}}{\sqrt{g}} \right\rangle / \left\langle \frac{g_{\theta\theta}}{\sqrt{g}} \right\rangle = \frac{1}{r^2} \quad (40)$$

Ultimately the source of tearing mode depends on the perturbation of the physical current density near the rational surface, which is related to the contravariant toroidal current by  $J_{0\phi} = \sqrt{g_{\phi\phi}} J_0^\phi$ , where  $\sqrt{g_{\phi\phi}} = R$ :

$$J_{\phi,1} \equiv J^* \propto \frac{J_{0\phi}}{T} R \quad (41)$$

Near the rational surface  $r = r_s$  the strength of driving term of the tearing perturbation in eq. 37 in the present test case can be explicitated as:

$$J^* = -AR^2 - BR^4 \quad (42)$$

where the equilibrium current used here is given by the expression consistent with eq.21 and  $A = \frac{P_0}{T}$ ,  $B = \frac{\Omega}{T}$ . In the next section, for the sake of argument, we focus on the scaling of the current perturbation with the characteristics of this equilibrium, which, albeit particular (eqs.21,23), keeps track of the fundamental toroidal metrics underlying also any more detailed equilibrium current profile. As argued earlier it is worth searching how the associated information may be linked to the stability condition.

#### A. Multipolar moments of Tearing Current Density Perturbation

In this section we shall investigate whether a generic tearing current perturbation " $J^\Delta$ " leaves a specific, and detectable, multipolar "footprint" on an outer contour (e.g. LCMS), and construct applicable, albeit approximate expressions. We can conjecture a scaling of the perturbation  $J^\Delta(r, \theta, \Omega) \propto AR^\lambda + BR^\nu$ , where the exponents  $\lambda, \nu$  are determined by the expected equilibrium current profile. A moment associated with the "tearing source"  $J^\Delta$  can be defined as:

$$Y^\Delta = \frac{1}{\mu_0 I} \oint f^\Delta B_\theta(r_b) dl = \frac{\psi'(r_b)}{\mu_0 I} \oint f^\Delta \frac{\sqrt{g_{\theta\theta}(r_b)}}{\sqrt{g(r_b)}} d\theta \quad (43)$$

From the general structure [9] of the  $f^{(m)}$ , solutions of  $\Delta^* f^{(m)} = 0$  it results that some linear combination of the functions  $f^{(1)}$ ,  $f^{(3)}$ ,  $f^{(5)}$  scaling as  $-\frac{1}{2R_0}R^2$ ,  $\frac{1}{4R_0^2}R^4$  and  $-\frac{15}{8}R^6$  can be useful to define a moment related to  $\Delta'$ :

$$f^\Delta \approx \alpha f^{(1)} + \beta f^{(3)} \approx -AR^\lambda - BR^\nu \quad (44)$$

In the specific case of eq. 41 we have  $\lambda = 2, \nu = 4$ . By matching the terms with corresponding powers of  $R$  in eq.44  $R^4$ , the constants are determined as  $\alpha = -2R_0 \frac{P_0}{T}$ ,  $\beta = -4R_0^2 \frac{\Omega}{T}$  leading eventually to the practical definitions:

$$f_\Delta := -2R_0 \frac{P_0}{T} f_1 - 4R_0^2 \frac{\Omega}{T} f_3 \quad (45)$$

and from 43

$$Y^\Delta = -\frac{2R_0 \psi'(r_b)}{\mu_0 I} \oint \left[ \frac{P_0}{T} f_1 + 2R_0 \frac{\Omega}{T} f_3 \right] \frac{\sqrt{g_{\theta\theta}(r_b)}}{\sqrt{g(r_b)}} d\theta \quad (46)$$

Fig.1, and Fig.2 show the contour plots of the weight functions  $f_3$  and  $f_\Delta$ . It is expected that information of the internal "tearing source" is conserved in the mapping provided by the surface moments. A correspondence between the relevant measured moment and  $\Delta'$  can be established by numerical calculations, up to an irrelevant multiplication factor. Stability domains can be constructed in operating spaces  $(c_0, T)$  and  $(k, T)$  for different  $(m, n)$  modes and toroidal rotation  $\Omega$ . In order to test sensitivity, the strict choice of the source  $J^*$  model of eq.42 could be relaxed, with different  $\lambda, \nu$  leading to different linear combinations of  $f_m$ , which can show higher sensitivity to  $\Delta'$ . An example is discussed in the next section for  $\lambda = 4, \nu = 6$  and  $\hat{f}_\Delta := 4R_0^2 A f_3 + 8R_0^3 B f_5$ .

## V. SENSITIVITY AND STABILITY DOMAINS

The stability parameter  $\Delta'$  is calculated solving numerically the tearing equation 37., The results of the physical model are shown in Figs.3,4,5,6,7,8.

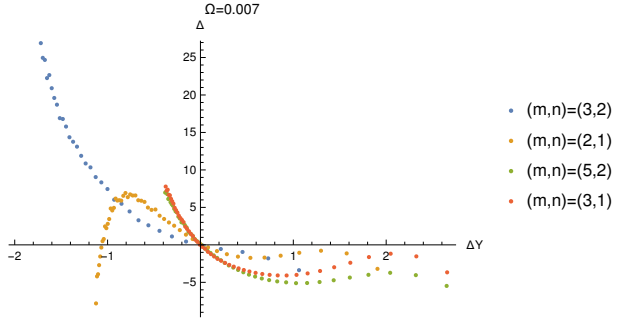


Fig. 3. Plot of  $\Delta$  vs.  $\Delta Y_{\Delta}$  for a range of modes  $(m,n)$  at a fixed value of the toroidal rotation label  $\Omega = 0.007$  (see definition 19);  $\Delta Y_{\Delta} \geq 0$  is associated with  $\Delta' \leq 0$

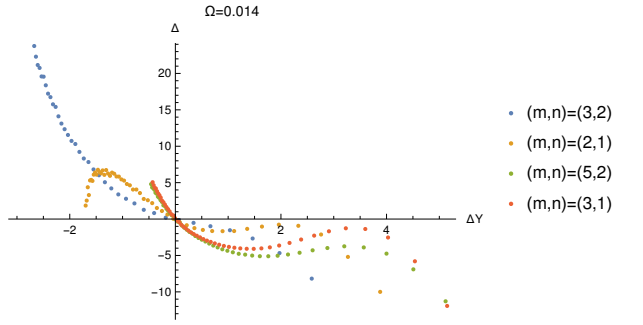


Fig. 4. Plot of  $\Delta$  vs.  $\Delta Y_{\Delta}$  for a range of modes  $(m,n)$  at a fixed value of the toroidal rotation label  $\Omega = 0.014$  (see definition 19)

The relation of the tearing linear instability parameter  $\Delta'$ , with the *externally measurable* moment  $\Delta Y_{\Delta} = Y_{\Delta} - Y_{\Delta=0}$ , for a range of modenumbers  $(m,n)$  is shown in 3,4, for two fixed values of rotation  $\Omega$ . The relation of  $\Delta'$  with  $\Delta Y_{\Delta} = Y_{\Delta} - Y_{\Delta=0}$ , for modes  $m = 2, n = 1$  and  $m = 3, n = 2$  is shown in Fig.5 and Fig. 6 for different values of the toroidal rotation  $\Omega$ . It is apparent that the change of sign of  $\Delta Y_{\Delta}$  is the same as that of  $\Delta'$ , irrespective of rotation: this makes this signal very suitable to monitor the (linear) stability condition.

It is possible to build the stability domains in the parameters space  $(c_0, k, T)$ . The analysis is done for  $m = 2, n = 1$   $k = 0.007, c_0 = 0.05, R_0 = 1.9, r_b = 1, \Omega = 0.007, p_0 = 0.1$  and the data are summarized in two contour plots.

The Figs.7,8 show that in the upper limit of the range of  $k$  and  $c_0$ , the moment  $\Delta Y_{\Delta}$  becomes larger, corresponding to a more stable equilibrium. This is consistent with the behaviour of  $\Delta'$  calculated using the exact equilibrium.

As a test of sensitivity to uncertainty in the basic structure of the  $J^*$  source, here we summarize the case with  $\lambda = 4, \nu = 6$  related to a different profile, *not consistent* with the equilibrium eq.23. The expression 46 is evaluated choosing, arbitrarily, the parameters  $m = 3, n = 2, k = 0.007, c_0 = 0.05, R_0 = 1.9, r_b = 1, \Omega = 0.007, p_0 = 0.1$ . The parameter  $T$  modifies

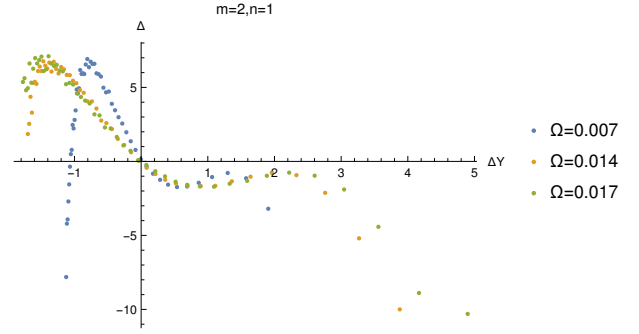


Fig. 5. Plot of  $Y_{\Delta}$  vs.  $\Delta Y_{\Delta}$  for mode  $m=2, n=1$  at different values of the toroidal rotation label  $\Omega$ ;  $\Delta Y_{\Delta} \geq 0$  is associated with  $\Delta' \leq 0$

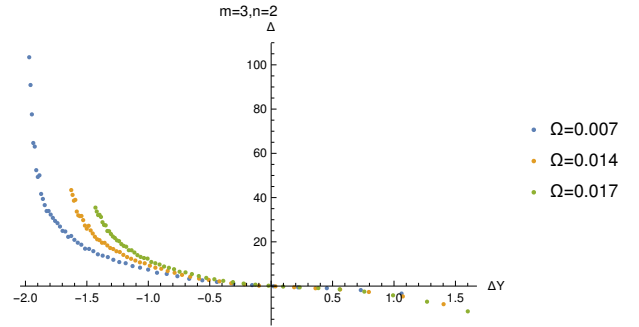


Fig. 6. Plot of  $Y_{\Delta}$  vs.  $\Delta Y_{\Delta}$  for mode  $m=3, n=2$  at different values of the toroidal rotation label  $\Omega$

only the profile of the safety factor  $q$ , in this way the geometry of the system is kept fixed. For each couple of values  $(c_0, k)$  the value of the  $Y_{\Delta=0}$  is calculated and subtracted from  $Y_{\Delta}$ . Note that in this case the sign of  $\Delta Y_{\Delta}$  is the same as that of  $\Delta'$ . In the table the sensitivity result is reported:

$T$	$\Delta'$	$Y_{\Delta'}$	$\Delta Y_{\Delta'}$
0.14	-0.0758541	-36.8296	0.
0.1	-3.37647	-52.5915	-15.7619
0.11	-1.80164	-47.8105	-10.9809
0.12	-0.947699	-43.8263	-6.99665
0.13	-0.55219	-40.455	-3.6254
0.14	-0.0758541	-37.5654	-0.735759
0.15	0.443696	-35.061	1.7686
0.16	1.12254	-32.8697	3.95991
0.17	1.87055	-30.9362	5.89342
0.18	2.61012	-29.2175	7.6121
0.19	3.28078	-27.6797	9.14986

It can therefore be confirmed that external magnetic measurements with rather flexible combinations of  $f_m$  multipolar weight functions can monitor the  $\Delta'$  stability condition.

## VI. SOURCE AND SIGNALS

In the previous sections of this paper the basic scaling of the metrics effect on the "tearing mode" current perturbation was inferred and it has been shown how a certain linear combination (*possibly not unique*) of the externally measurable  $Y_m$  is

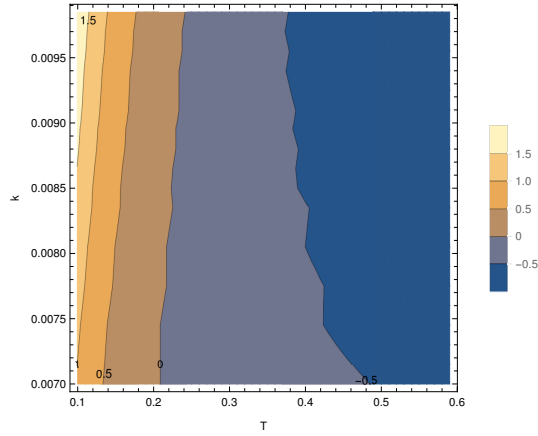


Fig. 7. Domain of stability identified by  $\Delta Y_{\Delta}$  vs.  $T, k$ . The region  $\Delta Y_{\Delta} \geq 0$  is stable

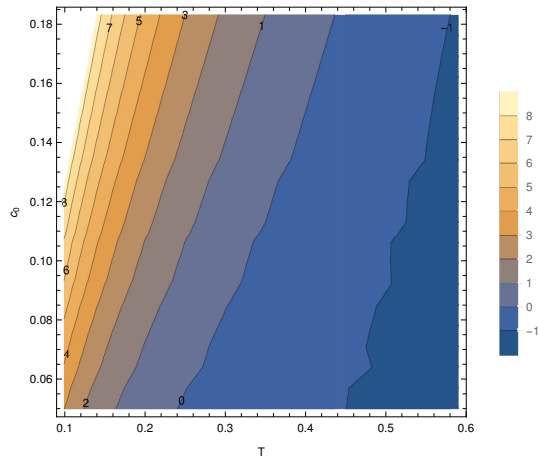


Fig. 8. Domain of stability identified by  $\Delta Y_{\Delta}$  vs.  $T, c_0$ . The region  $\Delta Y_{\Delta} \geq 0$  is stable

sensitive to the TM stability index  $\Delta'$ . An important question remains open, namely that concerning the detectability of this information amidst that provided by the other moments, and the background noise. To address this question, at least in a preliminary way, we have to introduce elements of information theory and of statistical decision techniques. For the specific purpose of modelling the "origin" of TM perturbations, to be "coded" onto externally measurable magnetic signals, because of the unknown non metrical effects, it is proposed to consider the current distribution as "source" of the multipolar moments  $Y_m$  defined in eq. 27, along the lines of ref. [9] as a set of independent random variables. One can consider a discrete subset of  $n$  generalized multipoles  $Z_i = \int \hat{J}_{\phi} L(f_i) dS_{\phi}$ , where  $L(f_i)$  is a linear combination more directly associated with physical quantities [8], [9]. The symbol  $Z_1$ , is associated with the Shafranov shift  $\Delta_{Sha}$ , while combinations  $Z_{\kappa} \approx L(Y_3, Y_4)$ , are associated with the elongation  $\kappa$ , and  $Z_{\delta} \approx L(Y_3, Y_6)$  are related with the triangularity  $\delta$  of the plasma configuration [9]; in the present case we are interested in  $Z_{\Delta} = \alpha Y_3 + \beta Y_5$ . On the basis of a statistical framework we can address the problem of assessing the detectability of the signal of interest.

### A. Statistical and probabilistic model

More specifically, we can picture the current as a "source" of  $n$  moments (eq.27) with amplitudes which are random variables described by "prior" probability distributions, taken, without loss of generality, to be Normal density distributions  $\Phi_N(Z_m | \mu_m, \sigma_m)$ , with mean  $\mu_m = Z_m$  and unspecified standard deviation  $\sigma_m$ . Then by reordering and subdividing the sequence  $Z_{min}, \dots, Z_m \dots, Z_{max} >$  we evaluate the probabilities of the "symbols"  $Z_m$  as :

$$P_1(-\infty \leq Z \leq Z_1) = \int_{-\infty}^{Z_1} \Phi_N(y) dy \quad (47)$$

$$P_k(Z_k \leq Z \leq Z_{k+1}) = \int_{Z_k}^{Z_{k+1}} \Phi_N(y) dy \quad (48)$$

$$P_m(Z_m \leq Z \leq \infty) = \int_{Z_m}^{\infty} \Phi_N(y) dy \quad (49)$$

In order to assess the relevance of the information of the symbol  $Z_{\Delta}$  in comparison with the other moments, here we follow a rather elementary line of reasoning.

We estimate the conditional probability that the message generated by the source is " $Z_{\Delta}$  when  $Z_{\kappa}$ " is also observed. The Bayes theorem gives the conditional probability

$$P(Z_{\Delta} | Z_{\kappa}) = P(Z_{\kappa} | Z_{\Delta}) \times P(Z_{\Delta}) / P(Z_{\kappa}) \quad (50)$$

Here  $P(Z_{\kappa} | Z_{\Delta})$  is the Likelihood function of detection of  $Z_{\Delta}$  when symbol  $Z_{\kappa}$  has been detected, and  $P(Z_{\kappa} | Z_{\Delta}) \times P(Z_{\Delta})$  is the "posterior" probability of symbol  $Z_{\Delta}$ , while  $P(Z_{\kappa})$  is the "evidence", which amounts to a normalization constant. Eventually by ordering the posterior probabilities, the relevance of the information of the  $Z_{\Delta}$  symbol can be assessed. In the language of information theory, the ensemble of  $Z_i$  is the set of  $N$  "symbols", ("letters") of the "alphabet"  $A$ , of the "source" [17], which generates random variables each with a probability  $P_i$ . A string of "letters", "symbols" is an elementary event, "message" in a probability space and is a random process.

### B. Likelihood Ratio and Ideal Observer Analysis

We want to formulate the problem of detectability of a specific moment (symbol), say  $Z_{\Delta}$  in presence of at least another signal (message) [21], say  $(Z_1, Z_{\kappa}, Z_{\delta})$ ; in general one should consider detectability against background noise, but here, for the sake of argument, it is sufficient just the comparing between noiseless signals. The task is to discriminate between two classes of moments that can be measured; we label as "class 0" the set of symbols  $\mathbf{Z}_j$ , ( $j = 0, 1$ ) that do not include the information about  $\Delta'$ , and "class 1" that which does include it. The optimal discriminator of two classes of symbols, with probability densities  $p_j(\mathbf{Z}_j)$  is given by the Bayesian ideal observer [22], [23], expressed in terms of the Likelihood ratio (or the log Likelihood ratio) (see eq. 50). In the present case  $Z_{j,i}$ , ( $i = 1, n$ ) are samples of size  $n=4$  from normal density distributions  $p_j(\mathbf{Z}_j) = \Phi_N(\mathbf{Z}_j | \mu, \sigma)$ , with mean and variance  $\mu, \sigma$  determined by seeking maximum

Likelihood, for given "data"  $\mathbf{Z}_j$ , for each class  $j$ . The mean value and the value  $\hat{\sigma}^2$  that maximize the Likelihood function

$$L_n(\mathbf{Z}_j | \mu, \sigma) = \left( \frac{1}{\sqrt{2\pi}\sigma} \right)^n \exp \left[ -\frac{1}{2} \frac{\sum_{i=1}^n (Z_i - \mu)^2}{\sigma} \right] \quad (51)$$

turn out to be :

$$\hat{\mu} = \bar{Z} = \frac{1}{n} \sum_i Z_i, \quad \hat{\sigma}^2 = \frac{1}{n} \sum_i (Z_i - \hat{\mu})^2 \quad (52)$$

$$L_n(\hat{\mu}, \hat{\sigma}) = \left( \frac{1}{\sqrt{2\pi}\hat{\sigma}} \right)^n e^{-\frac{n}{2}} \quad (53)$$

For class 0,  $\hat{\mu} = \mu_0$  and for class 1  $\hat{\mu} = \mu_1$ . The likelihood ratio statistic is defined as:

$$\Lambda(\mu, \sigma) = \frac{L_{n,0}(\mathbf{Z}_0 | \mu_0, \sigma_0)}{L_{n,1}(\mathbf{Z}_1 | \mu_1, \sigma_1)} = \left( \frac{\sigma_1^2}{\sigma_0^2} \right)^{\frac{n}{2}} = \left( \frac{\sum_i (Z_i - \bar{Z})^2}{\sum_i (Z_i - \mu_0)^2} \right)^{\frac{n}{2}} \quad (54)$$

As particular test case we consider the discrimination of a "message" string of length  $n=6$ , including the  $Y_4$  moment, associated with elongation, and no  $Z_\Delta$ , and one with  $Z_\Delta$  in place of  $Y_4$ . The sample means are  $\mu_0 = \frac{1}{n}(Y_1 + Y_2 + Y_3 + Y_4 + Y_5 + Y_6)$ ,  $\mu_1 = \frac{1}{n}(Y_1 + Y_2 + Y_3 + Z_\Delta + Y_5 + Y_6)$ . We can apply the analysis formulating the null hypothesis  $\mathbf{H}_0$  in relation to the detection of the value of one parameter, typically the mean,  $\mu_0$ , of the  $p_0$  distribution and the alternative  $\mathbf{H}_1$  associated with  $\hat{\mu} = \mu_1 \neq \mu_0$ . Intuitively, if the evidence (data) supports  $\mathbf{H}_1$ , then the likelihood function  $L_{n,1}(\mathbf{Z}_1 | \mu_1)$  should be large, therefore the likelihood ratio  $\Lambda$  is small. Thus, the null hypothesis  $\mathbf{H}_0$  is rejected and the symbol  $Z_\Delta$  is detectable. The rejection region for  $\mathbf{H}_0$  (acceptance for  $\mathbf{H}_1$ ) is  $\Lambda \leq \hat{k}$ , which is some threshold, and after some manipulation of eq.54, is translated into a t-Student test criterion for the statistics  $t = \sqrt{n}(\bar{Z} - \mu_0)/S > \hat{k}'$ , with the standard deviation estimator  $S^2 = \frac{1}{n-1} \sum_i (Z_i - \mu_0)^2$ . The level of significance of the null hypothesis at 5% occurs if  $t > 1.96$ .

$\mu_0$	$\mu_1$	$\sigma_0$	$\sigma_1$	$S$	$t$
-0.495	-0.081	1.40	0.963	0.43	2.35

Furthermore, another discriminating parameter is the distance of the peaks of the posterior density functions, divided by the standard error estimate  $d' \equiv \frac{\mu_1 - \mu_0}{S} \approx 0.422$ . Hence the moment  $Z_\Delta$  should be reasonably observable in an experimental situation, even in presence of the measurements of the other moments, typically the moments associated with the elongation. A plot of prior and posterior probability distributions (ref.50) for  $Y_4$  and  $Y_\Delta$  is shown in Figs.9,10. By construction, it is clear that the discriminating effect is due to rotation, even though the change of sign of  $Y_\Delta$  with  $\Delta'$  appears largely independent of rotation, for all modes.

Other combinations of moments such as  $\hat{f}_\Delta$  presented previously, monitor as well the sign of  $\Delta'$ , and are more detectable. This indicates a sufficient freedom for applications.

## VII. CONCLUSIONS

A new approach has been presented to the problem of detection of meaningful characteristics of a tokamak configuration, based on the simplest, but fully toroidal model of

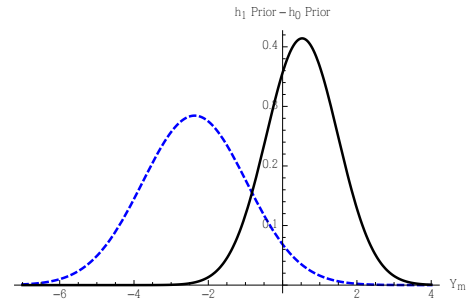


Fig. 9. Prior probability distributions of  $Y_4$  and  $Z_\Delta$  for  $H_0$  and  $H_1$

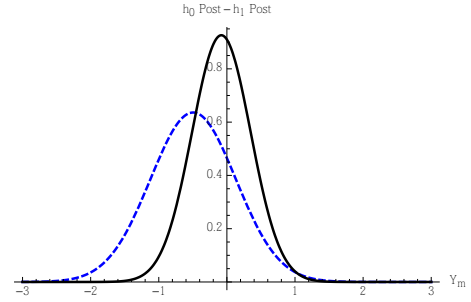


Fig. 10. Plot of posterior probability distributions of  $Y_4$  and  $Z_\Delta$  for  $H_0$  and  $H_1$

equilibrium, Solov'ev-like, but with rotation. The detectability of the sign of  $\Delta'$  is clearly due to an effect of rotation. Exploiting the vacuum solution of the field equation in terms of Legendre functions, some new, relevant information on the tearing stability conditions has been shown to be associated with combinations of *externally measurable* multipole moments. The choice of combinations is not unique, but several can be sensitive to the sign of  $\Delta'$ . By a statistical approach a procedure of Bayesian inference has been used to ascertain "theoretical" detectability of the relevant multipole moment. Given the simplicity of the assumptions, the procedure can be applied to more refined theoretical models and, especially, can be tried on real experimental measurements, where no detailed knowledge of the internal current profile is available.

## APPENDIX

Evaluation of Coefficients of the Parametric Representation

The solution eq.23 can be usefully represented in the general parametric form [3], in a mildly non uniform current approximation

$$R(r, \theta) = R_{ax} + (\epsilon R_1 + \epsilon^2 R_{11}) \cos \theta + \epsilon^2 R_2 \cos 2\theta - \delta \epsilon^2 \quad (55)$$

$$Z(r, \theta) = (\epsilon Z_1 + \epsilon^2 Z_{11}) \sin \theta \quad (56)$$

with  $\epsilon \sim \frac{r}{R_0}$  is an ordering tag, eventually set to 1. A system of equations can be built evaluating the moments of the solution  $\psi(R(r, \theta), Z(r, \theta))$ :

$$\int_0^{2\pi} \epsilon^2 \bar{\psi} \cos n\theta d\theta = \int_0^{2\pi} [c_0 R^2 Z^2$$

$$+k(R^2 - R_0^2)^2 + \frac{\Omega\psi}{24}R^6 - \psi_{ax}] \cos n\theta d\theta \quad (57)$$

the term  $\bar{\psi}$  is now seen as a labelling variable which scales as  $r^2 \sim \epsilon^2$  and denotes a specific magnetic surface. The same order terms are equated to obtain the coefficients of the equations 55, 56.

$$R_1 = r, \quad R_{11} = -\frac{\Omega R_0^2 r}{32k}, \quad R_2 = \frac{r^2}{4R_0} \quad (58)$$

$$Z_1 = \frac{2\sqrt{2kr}}{\sqrt{c_0}}, \quad Z_{11} = \frac{\Omega R_0^2 r}{8\sqrt{2c_0k}}, \quad \delta = \frac{3r^2}{4R_0} \quad (59)$$

Further steps are needed to ensure that the LCMS remains fixed. The boundary conditions have to be imposed:

$$R(r_b, 0)|_{\Omega=0} = R(r_b, 0), \quad R(r_b, \pi)|_{\Omega=0} = R(r_b, \pi) \quad (60)$$

$$Z(r_b, \frac{\pi}{2})|_{\Omega=0} = Z(r_b, \frac{\pi}{2}), \quad \beta_p|_{\Omega=0} = \beta_p \quad (61)$$

The coefficient  $k$ ,  $c_0$ ,  $R_0$  and  $r_b$  are functions of toroidal flow  $\Omega$ . The system is solved after a linearization of these coefficients:

$$k = k_0 + \epsilon k_1, \quad R_0 = R_{00} + \epsilon R_{01} + \epsilon^2 R_{02} \quad (62)$$

$$c_0 = c_{00} + \epsilon c_{01}, \quad r_b = r_{b0} + \epsilon r_{b1} \quad (63)$$

So, the system yields:

$$R_{00} = R_0, \quad R_{01} = \frac{\Omega R_0^3}{32k}, \quad R_{02} = \frac{(7c_0 + 24k)\Omega^2 R_0^5}{2048k^2(c_0 + 8k)} \quad (64)$$

$$c_{00} = c_0, \quad c_{01} = \frac{c_0 \Omega R_0^2}{2c_0 + 16k} \quad (65)$$

$$k_0 = k, \quad k_1 = -\frac{(c_0 + 4k)\Omega R_0^2}{8(c_0 + 8k)} \quad (66)$$

$$r_{b0} = r_b, \quad r_{b1} = \frac{\Omega r_b R_0^2}{32k} \quad (67)$$

Using 58,59 and 64-67, the final form of the parametric representation 55 and 56 can be written as:

$$R(r, \theta) = R_0 + \epsilon r \cos \theta - \epsilon^2 \frac{r^2 (8 \sin^2 \theta - \cos 2\theta + 3)}{4R_0} - \epsilon^2 \frac{\Omega r R_0^2 \cos \theta}{32k} \quad (68)$$

$$Z(r, \theta) = \epsilon \frac{2\sqrt{2}\sqrt{kr} \sin \theta}{\sqrt{c_0}} + \epsilon^2 \frac{\sin \theta (64kr^2 \cos \theta - \Omega r R_0^3)}{8\sqrt{2c_0k}} \quad (69)$$

From the equations 68 and 69 one can calculate the metric tensor used in eqs.37 and 46.

#### ACKNOWLEDGMENT

This work has been carried out within the framework of the EUROfusion Consortium and has received funding from the Euratom research and training programme 2014-2018 and 2019-2020 under grant agreement No 633053. The views and opinions expressed herein do not necessarily reflect those of the European Commission

#### REFERENCES

- [1] L.S. Solov'ev. Journal of Experimental and Theoretical Physics, **26** 400, (1968).
- [2] H. Tasso e G. N. Throumoulopoulos, Physics of Plasmas **5** 2378-2383, (1998).
- [3] L. Lao, Hirshman, Wieland, The Physics of Fluids **24**, 1431 (1981).
- [4] V. D. Shafranov, Plasma Physics, **13**, pp. 757 to 762.
- [5] L.E.Zakharov, V.D. Shafranov, Zh. Tekh. Fiz., **43**, 225 (1973).
- [6] A. J. Wootton, Nucl. Fusion **19**, 987 (1979).
- [7] M.F. Reusch, G.M. Neilson J. Com. Phys., **64**, 89 (1982).
- [8] I. P. Shkarofsky, The Physics of Fluids **25**, 89 (1982);
- [9] Seong-Heon Seo et al. The Physics of Plasmas **7**, 1487 (2000).
- [10] A. Tautz, I. Lerche. Astronomy and Astrophysics **A6**, 581 (2015).
- [11] R.D.Jackson, *Classical Electrodynamics*, Wiley (1962).
- [12] N.N.Lebedeve, *Special Functions*, Dover (1962).
- [13] J. Blum, E. Lazzaro, J. O'Rourke, B. Keegan and Y. Stephan Nucl. Fusion **30** 1475 (1990).
- [14] F. Alladio and F. Crisanti, The Physics of Fluids **26**, 1143 (1986).
- [15] E. Lazzaro, P. Mantica, Nucl. Fusion, **28**, 913 (1988)
- [16] Shannon, C.E., "A mathematical theory of communication," Bell System Technical Journal, **27**, pp. 379-423; pp. 623-656. (1948).
- [17] Khinchin A.I., *Mathematical Foundations of Information Theory*, Dover (1963)
- [18] Pierce, *An introduction to Information Theory*, DoverPub. Inc, New York (1980)
- [19] Kullback S., Leibler R.A., Annals of Mathematical Statistics, **22**(1), 79-86 (1951)
- [20] Galas D.J., Dewey J., et al, Axioms 2017, 6(2), 8; <https://doi.org/10.3390/axioms6020008> - 01 Apr 2017
- [21] Senfong Zheng, Lecture notes
- [22] Nghia Q Nguyen, Craig K Abbey, Michael F Insana, Proceedings of 2011 IEEE International Ultrasonics Symposium
- [23] H.H.Barrett, K.J. Myers *Foundations of Image Science*, Hoboken, NJ, John Wiley Sons (2004).

**Enzo Lazzaro** Plasma physics theorist, presently Associate Research Director of ISTP-Cnr. Formerly Director of Institute of Plasma Physics-CNR. From 1981 to 1990 researcher in the Theory Division of JET-Joint Undertaking and since then actively involved in plasma theory (wave-plasma interactions, MHD and dusty plasma) related to Tasks of Eurofusion and and other international collaborations, authoring and co-authoring about 300 papers.

**Luca Bonalumi** MSc Degree in Plasma Physics from Universit di Milano -Bicocca in 2019

**Dr. Silvana Nowak** is presently First Reasearcher at ISTP-CNR; she has worked at CEA (France) and JET (UK) and is currently involved in several Tasks of Eurofusion and other international collaborations.

**Dr. Daniele Brunetti** got his Msc Degree at the Universit degli Studi di Milano, and later his PhD at EPFL in Lausanne (SW); he has worked onl Tasks of Eurofusio at JET and is currently Reasearcher at CCFE, Culham, UK.